**PAPER** • **OPEN ACCESS**

# Enhanced pressure & proximity sensitivities of a flexible transparent capacitive sensor with PZT nanowires

To cite this article: L Pang *et al* 2019 *IOP Conf. Ser.: Mater. Sci. Eng.* **479** 012035

View the article online for updates and enhancements.



IOP ebooks™

Bringing you innovative digital publishing with leading voices to create your essential collection of books in STEM research.

Start exploring the collection - download the first chapter of every title for free.

This content was downloaded from IP address 120.79.214.236 on 17/09/2019 at 10:58

# Enhanced pressure & proximity sensitivities of a flexible transparent capacitive sensor with PZT nanowires

**L Pang, Q L Zhao[1], T Y Sheng, G P He, J J Di, T T Su and P P Tan**

School of Mechanical and Material Engineering, North China University of Technology, Beijing 100144, China

[1] E-mail: zql-01@163.com

**Abstract**. Capacitive pressure & proximity multi-function sensors are wildly used in applications such as 3D touch screen and electronic skin. However, those sensors could not meet rigorous requirement for accurate quantitative monitoring due to the lower permittivity of the dielectric material. $Pb(Zr_xTi_{1-x})O_3$ (PZT) material is featured in remarkably high dielectric constant. Here in this work, we present a flexible, transparent capacitive proximity & pressure multi-function sensor with PZT single crystal nanowires (NWs) and polydimethylsiloxane (PDMS) composite as dielectric layer. Experimental results confirmed the perovskite lattice structure. The length of the nanowires is about 50-100 μm, with diameter in magnitude of hundred nanometers. The sensor with PZT NWs could yield excellent pressure sensitivity for nearly 89 $MPa^{-1}$, which is about 10 times larger than that of the one only with PDMS dielectric layer. The proximity sensing property was also improved with adding PZT NWs in PDMS dielectric layer. Therefore, the performance of our sensor was significantly improved by the utilization of PZT NWs. And such kind of techniques could also be contributed to the development of practical applications like human-machine interface and distance monitoring systems.

## 1. Introduction

Types of sensing functionalities were realized based on capacitive sensing technology, pressure & proximity sensing are wildly used ones. Compared with other principles, capacitive sensing shows advantages of simple structure requirements, good immunity to temperature change, excellent dynamic response and low energy consumption. Capacitive sensors have been one of the most economical and viable solutions, especially for the integration of tactile and proximity sensing capability deployed in robot application [1]. However, as the requirement for accurate quantitative monitoring is getting more rigorous, those sensors with lower sensitivity could not meet that due to the lower permittivity of the dielectric material.

Another notable trend is that polymers are being introduced into capacitive sensing, which endowed the sensor with more features, such as transparency, flexibility, etc. Lots of efforts have been made to create new kind of capacitive pressure & proximity multi-function sensors. For example, Tsuji and Kohama [2] proposed a transparent sensor that could be used as a 3D touch screen. Capacitive transduction method is also undergoing rapid development to meet new opportunities of electronic skin [3]. Polydimethylsiloxane (PDMS), as a commercially available silicone rubber with a wide range of applications [4], is especially favorable because of its optically transparency, inert, non-toxic, and non-flammable. With good mechanical compatibility of the elastic support layer, it is also desirable to use PDMS directly as the dielectric layer [5].

Content from this work may be used under the terms of the Creative Commons Attribution 3.0 licence. Any further distribution of this work must maintain attribution to the author(s) and the title of the work, journal citation and DOI.
Published under licence by IOP Publishing Ltd

Piezoelectric materials play a vital role in the fields of electrical, ultrasonic, energy conversion, and many others due to their inherent peculiarity [6]. For instance, $Pb(Zr_xTi_{1-x})O_3$ (PZT) material is featured in remarkably high relative dielectric constant $\varepsilon_r$ (around several hundreds to thousands), which is much larger than that of PDMS ($\varepsilon_r$ ~2.8). Wide ranging application of PZT have also attracted considerable attention in the field of nanotechnology. As a representative structure, PZT nanowire (NW), as well as PZT nanoparticle [7-10], have been extensively explored to improve mechanical flexibly [11] of the relevant devices. There are some methods to prepare PZT nanowire, such as pulsed laser deposition [12], electrophoresis [13], hydrothermal [14], etc. It indicates that hydrothermal method is a feasible way to be undertaken in terms of high productivity. With the basic constituents of PZT NW and PDMS, it is possible to integrate nanotechnology with capacitive sensing method to enhance the sensitivity of pressure & proximity sensor.

Here in this work, we present a flexible, transparent capacitive proximity & pressure multi-function sensor with PZT single crystal nanowires and PDMS composite as dielectric layer. PZT NW was synthesized by a 2-step hydrothermal process [15]. Morphology of the nanowire was observed by subsequent characterization and single crystal perovskite structure was also be confirmed. PDMS/PZT NW layer prepared by spin-coating process plays a pivotal role on proximity & pressure sensing. The sensor has a sandwich structure owing to its ease of preparation and low cost. The Experimental results show that the performance of our sensor was significantly improved because of the utilization of PZT NW, as we demonstrate in the follow.

## 2. Experimental

Figure 1 (a) is a decomposition view of the sandwich-structure sensor. Figure 1 (b) illustrates the flow chart of the fabrication procedure. First, 20μm-width ITO electrodes on PET substrates were fabricated by photolithography and wet etching technologies. Next, PZT NWs were added into PDMS (10:1 ratio of PDMS base to curing agent). Mass ratio of the compound was 6 milligrams per gram PDMS. After stirring for an hour, the PZTNW/PDMS compound was uniformly spin-coated (1000 rpm, 30 s) on a pair of PET sheets. Make sure that compound was applied on the surface with ITO patterns. In order to expel those air bubbles in the compound, PET sheets experienced vacuum drying at 80 ℃ for 2 h. Then, pick out one of the sheets and spin-coated again because the compound could also serve as adhesive. While bonding, notice that the parallel electrodes on the top substrate should be perpendicular to those on the bottom substrate to get a matrix-structure sensor. Finally, vacuum drying with the aforementioned conditions was conducted. We also prepared a reference device in the same condition except that PZT NWs were not added in PDMS.

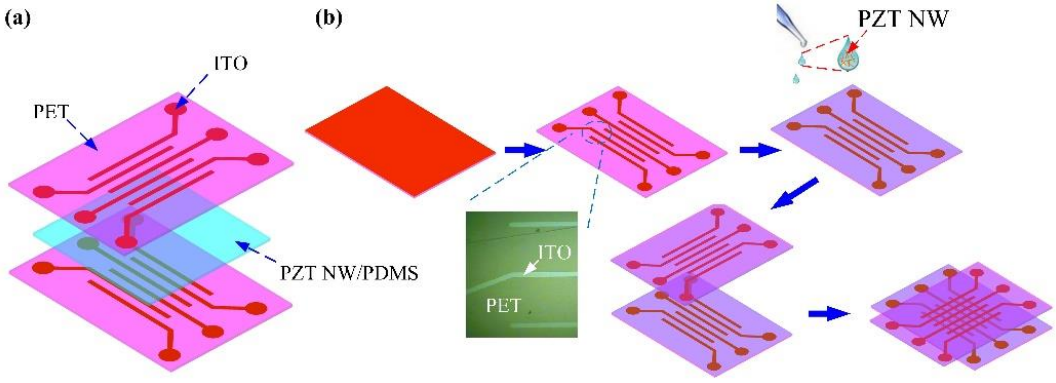



**Figure 1.** (a) Structure and (b) fabrication flow chart of capacitive pressure & proximity multi-function sensor.

PZT NW is the vital ingredient of our sensor. A 2-step hydrothermal approach was employed. The procedure of step one is as follows: First, tetrabutyl titanate ($[C_4H_9O]_4Ti$) water solution was prepared, then mixed with zirconium oxychloride ($ZrOCl_2 \cdot 8H_2O$) ethanol solution under stirring. Molar ratio of

Zr:Ti was set to 52:48. After ammonia had been added, white precipitation of $Zr_{0.52}Ti_{0.48}O(OH)_2$ (ZTOH) formed. The ZTOH was filtered and then dispersed into sodium hydroxide (NaOH) solution. The $TiO_2$ foil which served as substrate and the hydrothermal feedstock were placed into an autoclave for a hydrothermal treatment at 200 ℃ for 96 h. After cooling the autoclave to room temperature, the interim product bathed in ethanol, then washed with deionized water and finally dried in air.

When hydrothermal step two was conducted, the intermediate product was placed in autoclave together with potassium hydroxide (KOH) and lead nitrate ($Pb(NO_3)_2$). After heating at 200 ℃ for 2 h, PZT nanowire with PX phase was formed in dilute hydrochloric acid (HCl) soaking. At last, desired perovskite PZT NWs were converted by annealing the PX-PZT at 600 ℃ for 2 h.

## 3. Results & discussion

As shown in Figure 2 (a), all the peaks of the X-ray diffraction (XRD) pattern indicate the pure perovskite structure of $Pb(Zr_{0.52}Ti_{0.48})O_3$. Figure 2 (b) and (c) are the Scanning electron microscope (SEM) and transmission electron microscope (TEM) images of the NWs, respectively. The length of the NWs is about 50-100 μm, with diameter in magnitude of hundred nanometers. High resolution transmission electron microscope (HRTEM) image in Figure 2 (d) illustrates that the lattice spacing was measured to be about 0.28nm, which matches well with the available data of PZT aligned in [001] direction (PDF card No. 33-0784). Single crystal structure was detected by the corresponding selected area electron diffraction (SAED) pattern, as depicted in the inset.

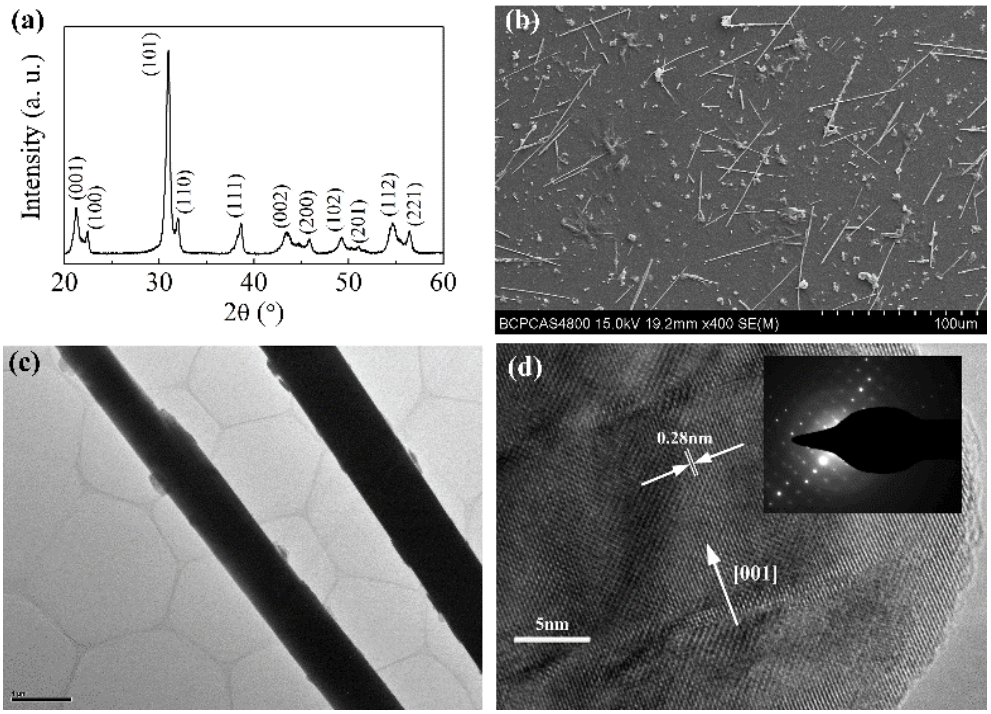



**Figure 2.** (a) XRD pattern of the PZT nanowires; (b) SEM and (c) (d) HRTEM images of the PZT nanowires. The inset in (d) is SAED pattern. The scale bar in (c) is 1 μm.

Figure 3 shows the transmittance spectra (Shimadzu, UV-3600) ranging in visible light and infrared. The transmittance could reach 80% at the wavelength of 600 nm. The left inset is the sensor in bended state. The right inset is a picture of the sensor with PZT NWs showing those background letters "NCUT", which is the acronym of North China University of Technology, could be clearly seen through the sensor. Marginal deviation between the two curves indicates neglectable effect on transparency caused by the utilization of PZT NWs.

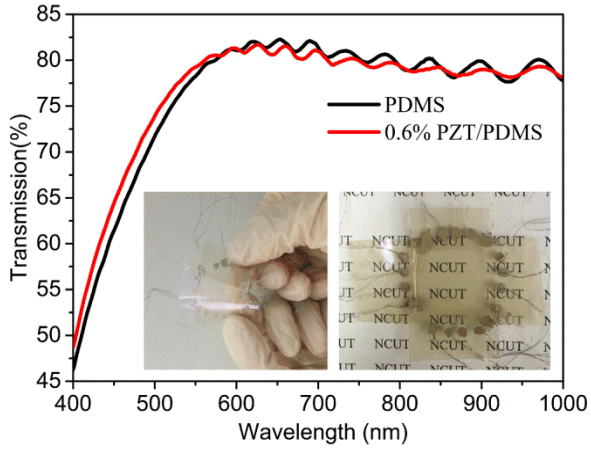



**Figure 3.** Transmittance spectra of sensors with and without PZT NWs. The insets are photographs of the sensor with PZT NWs.

One of the capacitor pixels was selected to be tested, as depicted in Figure 4 (a). Impedance analyzer (Keysight E4990A) was introduced to measure capacitance change. Applied voltage on the capacitor was 0.5 V for 200 kHz. Experimental data of pressure sensing was summarized in Figure 4 (b). Figure 4 (c) is the linear fitting result. Obviously, $\Delta C/C_0$ (rate of capacitance change) was linearly proportional to pressure in the low-pressure range. It is remarkable that the sensor with PZT NWs could yield excellent pressure sensitivity for nearly 89 $MPa^{-1}$, which is nearly 10 times and two orders larger than those of the ones only with PDMS dielectric layer (9 $MPa^{-1}$) in this work and reported in reference [16] (0.4 $MPa^{-1}$).

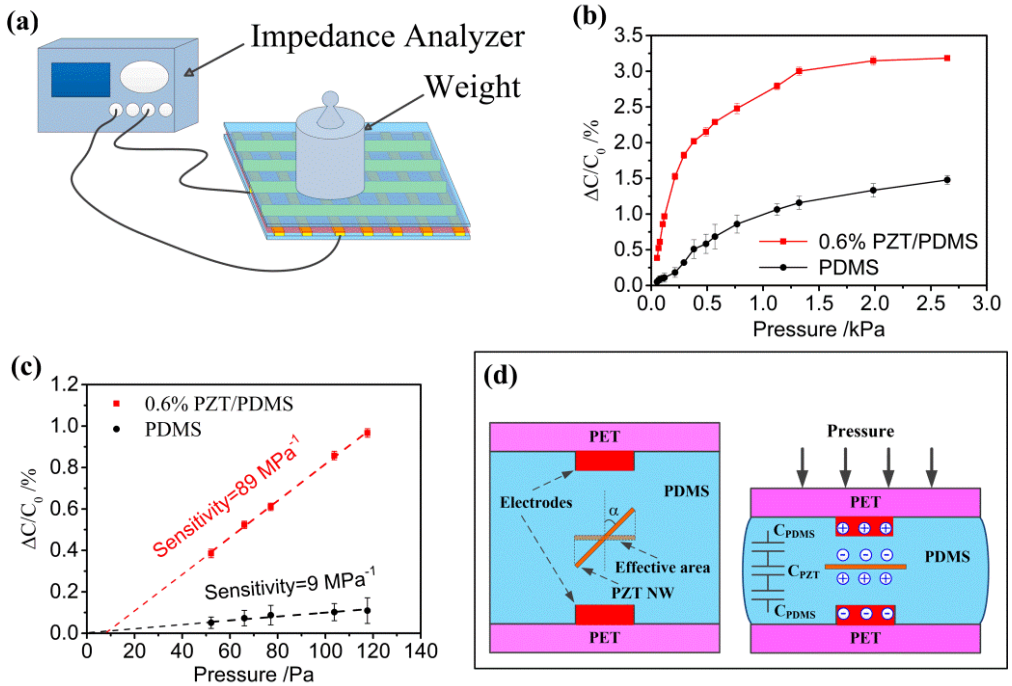



**Figure 4.** (a) Schematic diagram of the pressure sensing measurement; (b) experimental data of pressure sensing; (c) linear fitting result in the low-pressure range; (d) schematic diagram of the mechanism of the enhanced pressure sensitivity.

Suppose each of the ITO intersection of the $n \times n$ pixel matrix could be simplified as an individual parallel plate capacitor. According to the Hooke's law and the parallel capacitance equation, $\Delta C/C_0$ could be expressed by:

$$\sigma = SE = \frac{E \cdot (d_0 - d_1)}{d_0} = \frac{E \cdot \Delta d}{d_0} \tag{1}$$

$$\frac{\Delta C}{C_0} = \frac{\frac{\varepsilon A}{d_1} - \frac{\varepsilon A}{d_0}}{C_0} = \frac{\varepsilon A}{C_0 d_0 (\frac{E}{\sigma} - 1)} \tag{2}$$

$$\sigma << E: \quad \frac{\Delta C}{C_0} = \frac{\varepsilon A \sigma}{C_0 d_0 E} \tag{3}$$

Where $\sigma$ and $S$ are the applied stress and strain. $E$ is the Young's module. $\varepsilon$ is the permittivity of dielectric material, $A$ is the plate area. $d_1$ and $d_0$ are the thicknesses of sensor with and without stress, respectively. Therefore, $\Delta C/C_0$ increases with the increasing of pressure as $E$, $\varepsilon$, and $A$ are considered to be constants. When the applied pressure is much smaller than the Young's module of elastic layer ($\sigma << E$), $\Delta C/C_0$ is linearly proportional to the applied pressure. The enhanced pressure sensitivity may be attributed to the rotation of the PZT NWs, as shown in Figure 4(d). The total capacitor could be considered as a series connection of capacitors $C_{PDMS}$ and $C_{PZT}$. According to the theory of parallel plate capacitor, capacitors $C_{PDMS}$ is proportional to the effective area of electrode plates when there is angle $\alpha$ between the random distributed PZT NWs and the vertical line which is perpendicular to surface of PET substrates. As a pressure is applied on the sensor, the length direction of PZT NWs will become horizon due to the lateral expansion of PDMS elastic layer and the capacitors $C_{PDMS}$ increase with increasing the effective area. Therefore, both the increase of effective area and the decrease of distance between of electrode plates contribute to the variation of $\Delta C/C_0$.

Figure 5 (a) shows the photographs of proximity sensing measurement. Capacitance reading could be distinctly decreased as the object (such as hand) approaches. As shown in Figure 5 (b), both $\Delta C/C_0$ decrease as the object coming into close and are well linear fitted below the distance of 5 cm. The proximity sensitivities are 0.24% $cm^{-1}$ and 0.2% $cm^{-1}$ for the sensors with and without PZT NWs, respectively. The proximity sensing property is slightly improved by adding PZT NWs in the PDMS elastic layer. It is worth noting that the values of $\Delta C/C_0$ are negative for proximity sensing while those are positive for pressure sensing. Therefore, the sensors could distinguish the proximity from pressure easily without confusion.

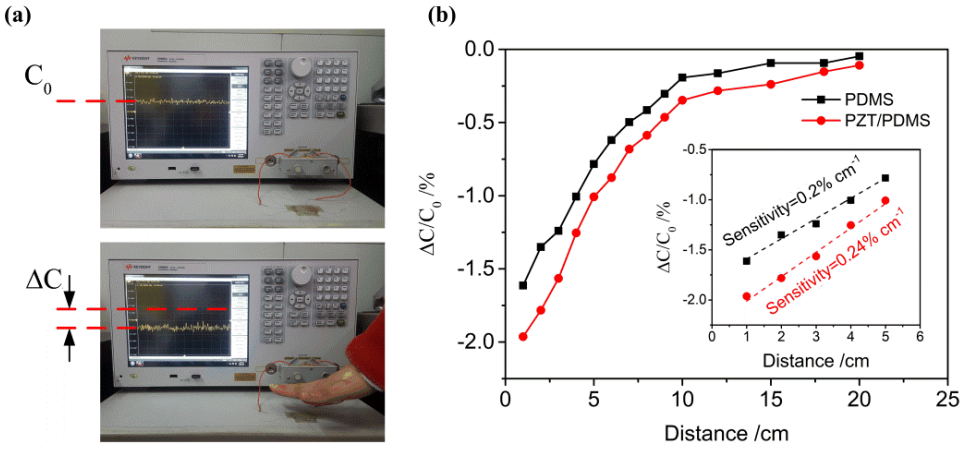



**Figure 5.** (a) Photographs of proximity sensing measurement; (b) experimental data of proximity sensing. The inset is the linear fitting result in the short distance range.

For the response mechanism of the proximity measurement, according to Zhang et al.'s theory [16], is based on a capacitive sensing scheme. Two types of capacitance, self-capacitance ($C_s$) and mutual capacitance ($C_m$) coexist in the device. It is reasonable to disregard the initial $C_s$, the capacitance of the ITO electrode stripe with respect to ground. Parasitic capacitance ($C_p$), which is related to the distance between the sensor and the approaching object with electrical conductivity, is the main factor that affects the capacitance measurement.

## 4. Conclusions

In this work, we proposed a flexible, transparent capacitive proximity & pressure multi-function sensor based on capacitance measurement. PZT NW was synthesized by a 2-step hydrothermal process. PDMS/PZT NW layer prepared by spin-coating process plays a pivotal role on proximity and pressure sensing. The experimental results show that the performance of our transparent sensor was improved by the utilization of PZT NW, especially for pressure sensing. It is desirable to undertake further developing on the matrix pixels and the corresponding circuit. Such kind of techniques could also be contributed to the development of practical applications like human-machine interface and distance monitoring systems.

## References

[1] Lee H K, Chang S I and Yoon E 2009 *IEEE Sensors Journal* **9(12)** 1748-55
[2] Tsuji S and Kohama T 2013 *SICE Annual Conference* 271-276
[3] Wang X, Dong L, Zhang H, Yu R, Pan C and Wang Z 2015 *Advanced Science* **2** 1500169
[4] Lötters J, Olthuis W, Veltink P and Bergveld P 1996 *Journal of Micromechanics & Microengineering* **7** 145-147
[5] Zhou S, Li M, Tang Q, Song Z, Tong Y and Liu Y 2017 *IEEE Electron Device Letters* **38(8)** 1031-34
[6] Ciofani G and Menciassi A 2012 *Piezoelectric Nanomaterials for Biomedical Application* Springer Berlin Heidelberg
[7] Park K, Jeong C, Ryu J, Hwang G and Lee K 2013 *Advanced Energy Materials* **3** 1539-1544
[8] Xu G, Ren Z, Du P et al 2005 *Advanced Materials* **17** 907-910
[9] Lin Y, Liu Y, Sodano H A 2009 *Applied Physics Letters* **95** 122901
[10] Xu S, Hansen B J, Wang Z L 2010 *Nature Communications* **1** 145-160
[11] Zhang G, Zhao P, Zhang X et al 2018 *Energy & Environmental Science* **11** 2046-56
[12] Chen Y, Liu T, Chen C et al 2012 *Acs Nano* **6(3)** 2826-32
[13] Yu L 2007 *Journal of the Chinese Ceramic Society* **35(6)** 782-785
[14] Lin Y, Liu Y and Sodano H 2009 *Applied Physics Letters* **95** 122901
[15] Wang J, Sandu C, and Setter N 2009 IEEE Transactions on Ultrasonics, Ferroelectrics and Freqency Control **56(9)** 1813-19
[16] Zhang B, Xiang Z, Zhu S et al 2014 *Nano Research* **7**(10) 1488-1496.